



Photocatalysis with nanostructured zinc oxide thin films: The relationship between morphology and photocatalytic activity under oxygen limited and oxygen rich conditions and evidence for a Mars Van Krevelen mechanism

Arshid M. Ali*, Emma A.C. Emanuelsson, Darrell A. Patterson*

Separation and Reaction Engineering, Department of Chemical and Materials Engineering, University of Auckland,
Private Bag 92019, Auckland Mail Centre, Auckland 1142, New Zealand

ARTICLE INFO

Article history:

Received 4 February 2010

Received in revised form 25 March 2010

Accepted 29 March 2010

Available online 3 April 2010

Keywords:

Zinc oxide

Nanostructured thin film

Photocatalyst

Methylene Blue

Magnetron sputtered

Mars Van Krevelen

ABSTRACT

The aim of this study was to evaluate the effectiveness of using a range of innovative nanostructured high surface area zinc oxide (ZnO) thin films as photocatalysts, and thereafter to systematically relate initial and reacted surface morphology and irradiated surface area to photocatalytic activity under both limited and rich oxygen conditions.

The thin films were produced using an innovative combination of magnetron sputtered surfaces and hydrothermal solution deposition that allows the morphology, porosity and thickness to be controlled by varying the composition and processing conditions. Methylene Blue (MB) was chosen as the model compound and the reaction was performed with ultra violet light (UV) at 254 nm. The thin film morphology and surface area before and after reaction was determined by scanning electron microscopy (SEM). The photocatalytic activity (measured as the rate and extent of MB degradation) was determined for seven different ZnO nanostructured thin films: three different ZnO hydrothermal solution depositions on bare glass slides (S1-CG, S2-CG and S3-CG films), the same three ZnO hydrothermal solution depositions but on glass slides coated with a magnetron sputtered ZnO film (S1-MS, S2-MS and S3-MS films), and glass slides coated with just a magnetron sputtered ZnO film (MS films).

A clear relationship between surface morphology (and the related thin film preparation method) and photocatalytic activity was observed for ZnO thin film supported catalysts: the tallest, most aligned structure had the highest photocatalytic activity, whilst the smallest, least aligned structure had the lowest photocatalytic activity. Thus, MB degradation rate was the fastest for the 1 µm thick ZnO thin film with a uniform arrayed structure from the S2-MS deposition technique. The degradation rates of the ZnO thin films were comparable to commercially available ZnO powder on a surface area basis. Photocatalytic degradation of MB under oxygen rich conditions increased for all other films except one film (S1-CG). This was most effective for thin film structure S2-MS, whose reaction rate was increased by 15%. Adding oxygen made the films more stable: in oxygen limited conditions, SEM and atomic absorption spectroscopy indicated zinc leaching had occurred. However, with additional oxygen the zinc leaching was minimised under the same reaction conditions. It is thought that this additional oxygen is either minimising the release of or replacing lost ZnO lattice oxygens, indicating that this ZnO photocatalytic oxidation could be occurring via a Mars Van Krevelen type redox mechanism.

© 2010 Elsevier B.V. All rights reserved.

1. Introduction

Metal oxides are one class of materials that have been successfully applied as photocatalysts, with applications ranging from self-cleaning windows to advanced oxidation processes for degrading bio-recalcitrant components in wastewaters. Currently, powder

titanium dioxide (TiO₂), and in particular Degussa P25, is the most the widely used, but zinc oxide (ZnO) and other metal oxide powders have also successfully oxidised a wide range of organic compounds. Moreover, ZnO has been found to have economic [1,2] and performance [1,3] advantages over titanium oxide for the degradation of certain compounds, including azo dyes. Some of the main problems however with powder catalysts are that they are hard to recover, recycle and separate, as well as producing potential health and environmental hazards [4]. To overcome these problems, much research has been focused towards supporting catalysts on rigid supports. These immobilisations can be achieved through

* Corresponding authors. Tel.: +64 9 373 7999; fax: +64 9 373 7463.

E-mail addresses: a.ali@auckland.ac.nz (A.M. Ali),
darrell.patterson@auckland.ac.nz (D.A. Patterson).

many deposition techniques, including sol–gel, hydrothermal solution deposition, spray pyrolysis and magnetic sputtering [5–7].

The major disadvantage with this is it that the resulting supported catalyst has a smaller surface area compared to the powder [8], which will result in a decreased catalyst activity, since halving the surface area of a heterogeneous catalyst typically halves the reaction rate [9]. This disadvantage can however be overcome if a predictable and robust nanostructured and therefore high surface area catalyst is used. Gao and researchers at the University of Auckland have developed a patented approach to make nanostructured ZnO thin film semiconductors using direct current magnetron sputtering, where the structure, porosity and properties can be controlled by the processing conditions [10,11]. This technique can prepare highly porous metal oxide films with a large surface area [9], providing the potential to overcome the limited surface area typically associated with supported catalysts. The disadvantage however is that the magnetron sputtered films are thin compared to other thin film formation methods, like sol–gel, and therefore the mass of catalyst and surface area per unit area of support is low. This paper therefore investigates using hydrothermal solution deposition [7] with these magnetron sputtered films as a template for growth in order to increase the mass and surface area of the catalyst whilst retaining the open, high surface area nano-sized surface structures and comparing this to thin films deposited without using the magnetron sputtered templates in order to determine if they are necessary to form the structures in the first place.

There have been a number of papers already published describing research into developing nanostructured powder and films and then comparing the photocatalytic activity with the surface area [12,13]. The general trend is as expected: an increase in surface area increases the photocatalytic activity of the metal oxides [12,14,15]. However, the 'smaller the better' is not always true, which is most likely due to a higher recombination rate of the electrons and holes (e^-/h^+) responsible for generating the radicals species that propagate the photocatalytic reactions in very small particles [13]. Another important factor for photocatalytic activity is the surface morphology, which several researchers suggest is more important than the surface area [16–21]. Most of the research effort in this area has however focused on metal oxide powders. For example, Wahi et al. [13] found that the photocatalytic degradation of Congo Red by TiO₂ nano-rods was slower than TiO₂ nano-dots. Although the nano-dots had a higher surface area, the difference was not sufficiently large enough to justify the large difference in activity. Wahi et al. [13] speculated that the difference could be attributed to the different water adsorption modes on the catalyst surface, caused by the crystal orientation. Li and Haneda [17] prepared a range of ZnO and found that for different ZnO powder samples prepared with the same methodology, the reaction rate was more affected by the crystallinity than the surface area. When comparing all samples, no correlation between either crystallinity or surface area to photocatalytic activity was obtained. However, when they compared the amount of absorbed substrate in comparison to photocatalytic activity divided by BET surface area to elucidate the effect of surface morphology, a linear relationship was observed. Li and Haneda [17] state that this suggests that the surface morphology is the most important factor for high photocatalytic activity. Furthermore Wang et al. [16] showed that ZnO dandelions had a higher photocatalytic activity than ZnO hollow spheres, nano-particles and nano-rods. These studies provide the foundation on top of which this work is built. This paper will extend this limited information on the relationship between film structure and photocatalytic activity, in particular elucidating these relationships for liquid-phase reactions for thin film catalysts.

As mentioned above, ZnO is not as widely used as TiO₂ and this is mainly because ZnO have shown to be less stable [22]. The reasons behind this instability have not yet been adequately studied. In par-

ticular, there is a lack of information on the surface structure before and after using metal oxide thin films in a photocatalytic reaction. Furthermore, no study has investigated how the oxygen concentration in the reaction affects the ZnO stability, and hence ultimately the reusability of thin film ZnO. Consequently, there is currently little understanding of the effects of oxygen concentration on the ZnO thin film microstructure. Additionally, by evaluating the photocatalytic activity under both limited and rich oxygen conditions, the effect of oxygen mass transfer on the reaction rate can be quantified. This is because the experiments with a limited oxidant supply (no added oxygen) allow comparison of the photocatalytic activity of the photocatalysts under the 'toughest' reaction regime, where the overall reaction rate could be mass transfer limited by the supply of oxidant.

Based on the above, the objectives of this study is to determine a relationship between initial and reacted catalyst morphology (such as surface area and structure) and photocatalytic activity for a range of ZnO thin films prepared by magnetron sputtering, hydrothermal solution deposition and a combination of the two [7,10,23]. To do this, this work will: (i) investigate the effect of oxygen concentration on the ZnO microstructure and photocatalytic activity, (ii) determine the effect of reusing the films in subsequent photocatalytic reactions on the ZnO microstructure and photocatalytic activity. This will be benchmarked against commercially available ZnO powder and ZnO magnetron sputtered nanostructured thin films.

2. Materials and methods

2.1. Materials

The following chemicals were obtained from Sigma–Aldrich (New Zealand): zinc nitrate hexahydrate ($\text{Zn}(\text{NO}_3)_2 \cdot 6\text{H}_2\text{O}$) 98%, polyethyleneimine (PEI) 50 wt% solution in water, 10% diluted ammonia solution (69%), 4% diluted nitric acid (70%), pure zinc metal and Methylene Blue (regent grade), synthesis grade hexamethylenetetramine (HMT) and microscope slides (7105 WT). Deionised water was used in all work. Zinc oxide powder used originated from the Beijing Mountain Technical Development Centre for Non Ferrous Metals in China.

2.2. Methods

2.2.1. Preparation of ZnO films

Four different ZnO morphologies were prepared via hydrothermal solution deposition growth. The substrate was either clean glass slides (henceforth referred to as 'clean glass film growth' or CG) or glass slides with an under layer of magnetron sputtered ZnO (henceforth referred to as 'magnetron sputtered template growth' or MS) with an approximate top surface area of $2\text{ cm} \times 1\text{ cm}$ (see Section 2.2.2 for evaluation method).

2.2.1.1. Magnetron sputtered template. For the magnetron sputtered template growth films, the glass substrate was loaded into the chamber of a custom made magnetron sputter film depositor [23]. When the deposition chamber was evacuated down to $\sim 5.3 \times 10^{-4}\text{ Pa}$, high purity argon was introduced into the chamber. Radio-frequency (13.56 MHz) power of 500 W was forwarded to the substrates to initialize the plasma for surface cleaning. After that, direct-current power was forwarded to a ZnO target (99.99%). Deposition was conducted for 30 min to establish a thin ZnO film on the glass substrate. This established a ZnO film template onto which further ZnO was deposited by hydrothermal solution deposition.

2.2.1.2. Hydrothermal solution deposition. Aqueous solutions for the growth of ZnO nano/microrods were prepared by mixing

Table 1
ZnO thin film preparation conditions.

	S1-MS	S1-CG	S2-MS	S2-CG	S3-MS	S3-CG
pH	5	5	7.5	7.5	5	5
Solution composition	$\text{Zn}(\text{NO}_3)_2$ + HMT	$\text{Zn}(\text{NO}_3)_2$ + HMT	$\text{Zn}(\text{NO}_3)_2$ + HMT + PEI	$\text{Zn}(\text{NO}_3)_2$ + HMT + PEI	$\text{Zn}(\text{NO}_3)_2$ + HMT + citrate	$\text{Zn}(\text{NO}_3)_2$ + HMT + citrate

80 mL each of 0.025 mol L^{-1} zinc nitrate and 0.025 mol L^{-1} hexamethylenetetramine (HMT) and 0.3 mL of 100% polyethyleneimine (PEI). Diluted nitric acid (4%) or diluted ammonium hydroxide solution (10%) was used to adjust the pH value to 5 or 7.5 to give a clear, colourless solution. The solution was then transferred into a sealable glass jar, in which the glass substrates were suspended vertically by using a corrugated Teflon support to achieve chemical deposition growth on one side of the substrate. The sealed jar was then put into an oven at 95°C for 4 h, after which the glass substrates were withdrawn from the solution, rinsed and wiped on the backside with deionised water, and then dried at room temperature [7]. Two different reaction conditions were used (see Table 1). The films obtained from solution S1 having composition $\text{Zn}(\text{NO}_3)_2$ + HMT on magnetron sputtered template growth and clean glass slides were designated S1-MS and S1-CG. Similarly the films obtained from solution S2 with $\text{Zn}(\text{NO}_3)_2$ + HMT + PEI on magnetron sputtered template growth and clean glass slides were designated S2-MS and S2-CG and the films obtained from solution S3 with $\text{Zn}(\text{NO}_3)_2$ + HMT + citrate on magnetron sputtered template growth and clean glass slides were designated S3-MS and S3-CG respectively.

2.2.2. Characterisation of ZnO films and powder

The surface and cross-sectional morphologies of ZnO thin films before and after photocatalytic reaction were characterized by scanning electron microscopy (SEM) using a Philips XL-30s operating at 5 kV. Both top surface and cross-sections were imaged. Cross-sectioning was carried out by cutting the thin film sample into two parts using wire cutters whilst holding it with pliers. A Polaron SC 7640 Sputter Coater was used to give a very thin, minimal Pt coating (600 s) suitable for SEM viewing. Total active surface area (S_{ex}) of the films (the surface area exposed to the UV light and therefore photocatalytically activated) was evaluated by measuring surface area of a random sample of a large number of the crystals obtained from both top view and cross-sectional SEM images, and then this was multiplied by the size of the glass substrates. The presence of Zn metal in the reacted sample was determined by atomic absorption spectroscopy (AAS) by using a Varian Spectra AA 50.

Surface area of the ZnO powder was determined by BET to be $35.7 \text{ m}^2 \text{ g}^{-1}$.

2.2.3. Photocatalytic degradation of Methylene Blue

Photocatalytic degradation experiments were performed in a custom made stainless steel UV reaction enclosure as shown in Fig. 1. The removable lid contained one 254 nm low pressure mer-

cury lamp with power supply (Davey Water Products, NZ). The enclosure was placed on top of two magnetic stirrers. The enclosure had side ports for in situ liquid sample removal and to allow the oxygen pipes to be fed from the gas cylinder to sparge the two beakers that were used as reaction vessel. The flow rate of oxygen was measured by using custom made gas bubble flow meter. Two reactions were run in parallel. The films were mounted horizontally into 100 mL beakers with the film side facing upwards. The film was secured in the centre of each beaker with Kanthal D wire. 40 mL of 5 mg L^{-1} Methylene Blue solution was then poured into each beaker. A magnetic stirrer was added and the beaker was placed inside the stainless steel enclosure.

Two repeats were conducted for each experiment and data is presented with error bars $\pm 5\%$ values. Prior to irradiation, Methylene Blue (Sigma–Aldrich, NZ) and ZnO films were allowed to equilibrate in the dark for 30 min. After this, UV-254 nm irradiation was carried out, having light intensity of approximately 0.83 mW cm^{-2} (measured by using an IL 1700 Radiometer) for 6 h at constant stirring speed. 0.8 mL samples were periodically withdrawn and the Methylene Blue concentration was evaluated by UV spectroscopy (Lambda 35 UV-visible PerkinElmer), measuring peaks at 662 nm (coefficient of variation 4%). Samples were then returned to the reactor so as to not change the overall reaction volume. Experiments with oxygen rich condition were performed at a flow rate of 5 mL s^{-1} by introducing oxygen when UV irradiation was initiated.

Experiments with ZnO powder were also performed at catalyst loading of 50 mg L^{-1} (since this was the lowest catalyst mass that could be accurately measured). Thin film suspension equipment was removed and the powder ZnO was loaded directly into the beakers. To perform analysis on the solution sample it was required to centrifuge liquid sample solutions at 2000 rpm for 2 min to remove ZnO particles.

Control experiments without ZnO thin film, ZnO powder and UV light were performed to baseline the Methylene Blue degradation in the absence of UV and photocatalysts and to determine the effect of water and UV alone on the ZnO thin films. These included, Methylene Blue solution in the dark, Methylene Blue solution irradiated with UV (photolysis), a ZnO thin film in deionised water in the dark, ZnO thin film without water irradiated by UV, and ZnO thin films in water irradiated with UV. The results of these showed no decolourization of the irradiated solution in the absence of photocatalysts, as well as no significant change in surface morphologies of the ZnO thin film. Four trial experiments at different oxygen flow rates (2, 3, 5 and 6 mL s^{-1}) were also conducted to ensure the saturation of reaction vessel with oxygen, determining that 5 mL s^{-1} was sufficient.

2.2.4. Data treatment and kinetic analysis

The Langmuir–Hinshelwood kinetic model was used to determine the reaction kinetics [24] (Eq. (1)), where C is the concentration of the reactant at any time t , N is the number of moles of reactant at any time t , k is the limiting reaction rate constant at maximum surface coverage of the reactant on the catalyst on a liquid volume basis, K is the reactant adsorption equilibrium constant, and V is the liquid volume in the reactor. At low concentrations $KC \ll 1$, and Eq. (1) can be simplified to Eq. (2), the first order rate equation, where k_{app} is the apparent first order rate constant. First

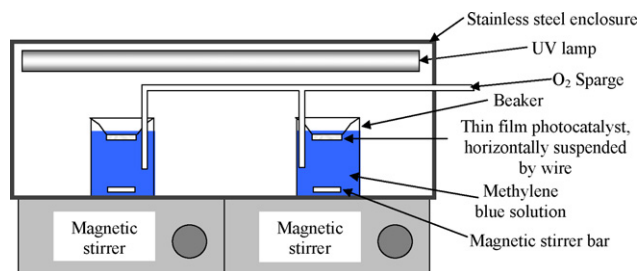


Fig. 1. Schematic of the experimental set-up of the photoreactor.

order degradation has been seen to occur in other studies [25–27], and consequently a first order kinetic analysis will be used here.

$$-\frac{dC}{dt} = -\frac{1}{V} \frac{dN}{dt} = \frac{kKC}{1+KC} \quad (1)$$

$$-\frac{dC}{dt} = -\frac{1}{V} \frac{dN}{dt} = k_{app}C \quad (2)$$

Eqs. (1) and (2) are in a liquid volume basis. However, since this does not account for any catalyst properties of the system (such as mass or surface area), the kinetic constants derived from these equations cannot be used to fairly compare the relative photoactivity of the different catalysts studied. Consequently, the kinetic parameters on a surface area basis will also be evaluated, where k'' and k'_{app} are the limiting reaction rate constant at maximum surface coverage of the reactant on the catalyst and the apparent first order rate constant on a catalyst surface area basis respectively (Eq. (3)):

$$-\frac{1}{S} \frac{dN}{dt} = \frac{k''KC}{1+KC} \approx k'_{app}C \quad (3)$$

S is the UV exposed surface area, since the reactions investigated are photocatalytic.

3. Results and discussion

3.1. Relationships with surface morphologies and thin film preparations

3.1.1. Morphology before reaction

Fig. 2 shows the SEM images for the cross-sections of the supported catalysts produced from the different preparation methods outlined in Table 1 before the reaction. For the S1 films (Fig. 2A and B), the surface morphologies for the template and clean glass slide growth display a different growth pattern, but similar sizes of ZnO deposits. Both S1-MS (Fig. 2A) and S1-CG (Fig. 2B) growth is characterised by relatively large ZnO rods (producing a film thickness of approximately 1.5–2 μm for S1-MS and 2–2.5 μm for S1-CG). The main difference is that for the MS template growth (S1-MS), the ZnO structure was more well aligned and arrayed, with single crystals growing up from the magnetron sputtered template (Fig. 2A). For the clean glass film growth (S1-CG), the ZnO columns aggregate together in random stacks both horizontally and vertically, as would be expected from growth that has no template to follow (Fig. 2B). For S1-MS, the magnetron sputtered under layer for S1-MS can be visualised (0.1–0.2 μm), but it is smaller than for the S2-MS (1 μm) films (Fig. 2C). This is most likely because the acidic growth conditions could have caused the magnetron sputtered under layer to partly dissolve. This means that it can no longer

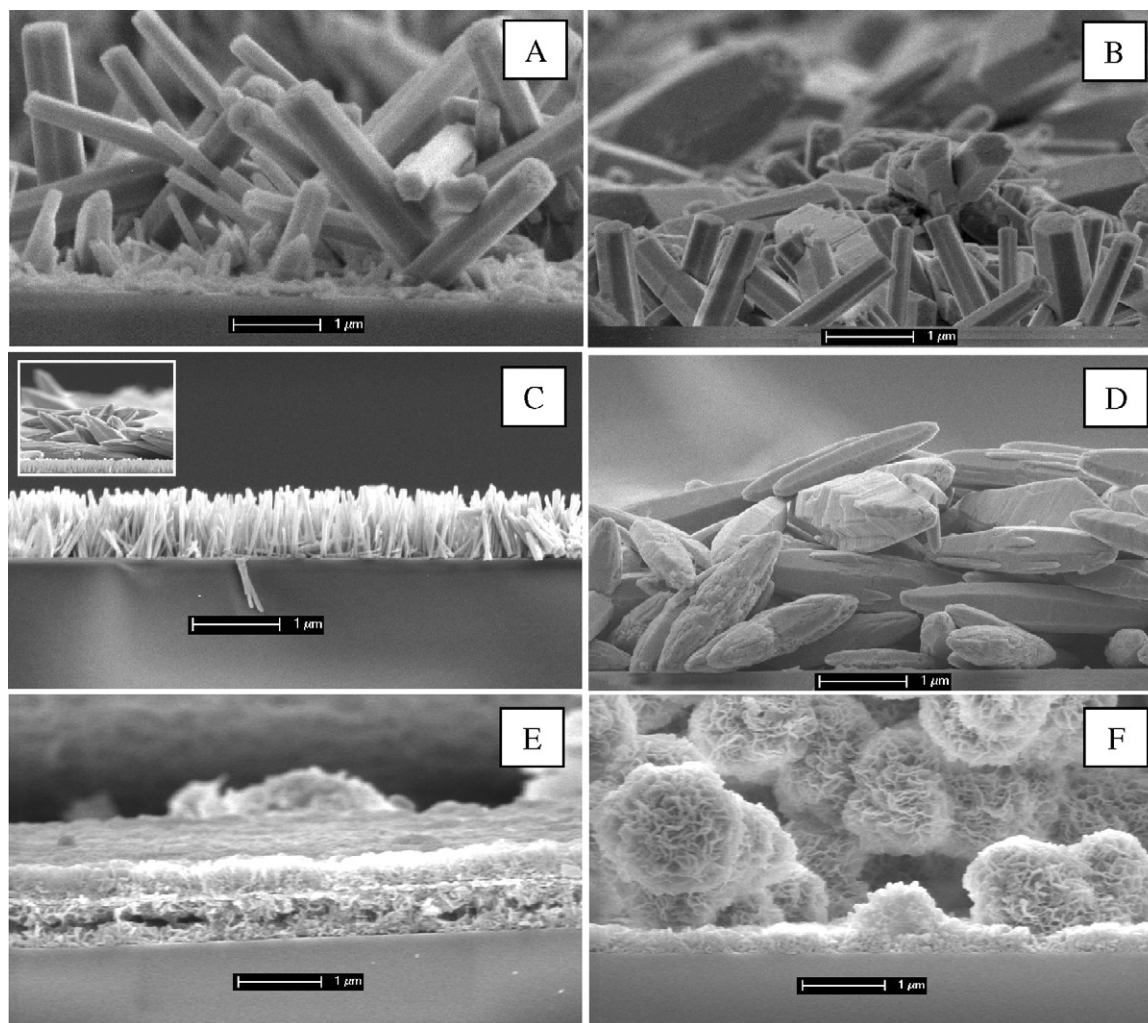


Fig. 2. Cross-sectional view of the surface morphologies of the different ZnO thin films before photocatalysis: (A) S1-MS; (B) S1-CG; (C) S2-MS (inset, an example of the large crystals that were sporadically present on the surface of the main structure); (D) S2-CG; (E) S3-MS; (F) S3-CG.

function as efficiently as a template for the size of growth, but still aligns the direction of growth, which explains the similar size but different alignment of the S1 structures.

For the second solution (S2; Fig. 2C and D), there is a marked difference in both size and direction of the ZnO crystal growth between the films resulting from template and clean glass slide growth. The S2-MS films (Fig. 2C) are characterised by smaller rods (about 1 μm tall) than the S1-MS. Also in Fig. 2C, the magnetron sputtered layer can be clearly observed, in contrast to that in Fig. 2A. This is because solution S2 has a neutral pH, the magnetron sputtered template hence remaining intact during the solution growth, giving rise to an orderly small structure. Note that on top of this small structure (Fig. 2C), there was a sparsely distributed ($\sim 2\text{--}5\%$) large structure, similar to S2-CG. For the S2-CG structure (Fig. 2D), the ZnO structures are larger (2–4.5 μm tall), with more random growth. Furthermore, the structure was not evenly distributed across the glass substrate.

For third solution (S3, Fig. 2E and F), there is also marked difference in both size and direction of ZnO crystal growth. S3-MS (Fig. 2E) has a considerably smaller (0.2–0.4 μm) fine flaky ZnO structure on top of magnetron sputtered layer than the other struc-

tures. The structure is similar to that which is expected when citrate is used in the hydrothermal solution deposition growth period [28]. In contrast, S3-CG (Fig. 2F) has a structure consisting of an aggregated stack of woven spheres that resemble a bunch of Genda flowers (1–1.5 μm) upon a highly dense three dimensional ZnO crystal structure. It has more uniform structure compared to S3-MS.

These structures are changed by the photocatalytic reaction with Methylene Blue, depending on the whether oxygen supplied is limited or rich, as shown in Figs. 3–5. These two conditions and the mechanistic implications of these results will therefore be outlined individually.

3.1.2. Morphology after reaction under limited oxygen conditions

Experiments with limited oxygen supply were initially performed to compare catalysts under the ‘toughest’ reaction regime, where the overall reaction rate could be mass transfer limited by the supply of oxidant. In this case, the only oxidant is from the dissolved oxygen within the liquid and additional oxygen can only be provided by mass transfer through the surface of the reaction liquid. Figs. 3B and E, 4B and E, and 5B and E, show how the surface structures for the six different films have changed after the pho-

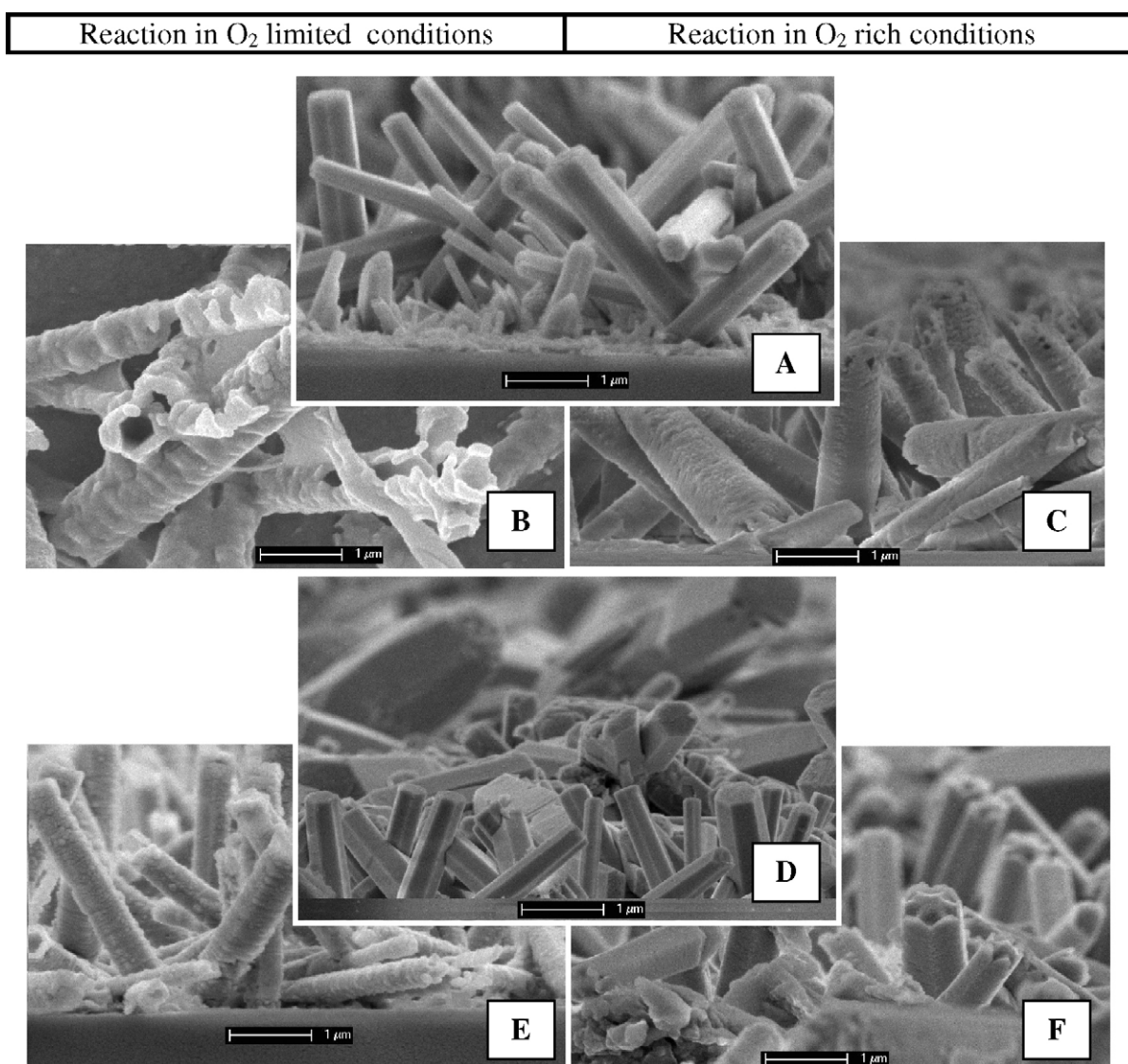


Fig. 3. Comparison of the solution 1 (S1) derived ZnO thin film surface morphologies using SEM imaging before and after Methylene Blue photocatalysed degradation: (A) S1-MS (un-reacted); (B) S1-MS (reacted with limited O_2); (C) S1-MS (reacted under O_2 rich conditions); (D) S1-CG (un-reacted); (E) S1-CG (reacted with limited O_2); (F) S1-CG (reacted under O_2 rich conditions).

photocatalysed reaction in oxygen limited conditions. Photocatalytic degradation of Methylene Blue did occur under these conditions at reaction rates comparable to those under oxygen rich conditions (see Sections 3.2 and 3.3 for details). However, it can be observed that the ZnO structures are severely affected by the photocatalytic oxidation, with significant degradation of all thin film structures in all reactions. SEM images show this very clearly. Prior to the reaction, the films (S1-MS, S1-CG, S2-MS and S2-CG) have intact solid columns of ZnO with smooth surfaces (Fig. 2A–D), S3-MS (Fig. 2E) has flakey ZnO structures and S3-CG (Fig. 2F) has a spherical woven structure as previously discussed. After the reaction, the columns have a rougher surface and some appear to be hollowed-out (Fig. 3B is an example of this), whereas S3-MS (Fig. 5B) shows that a layer of the ZnO thin film has been eroded away practically leaving the thin MS layer only, thus decreasing the thin film thickness. The component ZnO columns have also increased in size, perhaps through aggregation or a dissolution and recrystallisation process during

the reaction. This has overall caused a reduction its surface area. The spherical woven structure of S3-CG (Fig. 5D) is degraded into a more irregular woven structure through loss of parts of the ZnO structure.

As this degradation runs in parallel to a photocatalytic degradation of Methylene Blue that is comparable in terms of rate and extent of reaction to those in oxygen-rich conditions (see Section 3.2), the oxidant that is integral to the radical photocatalytic degradation mechanism must be being provided from some source in these reactions. Based on the erosion of the thin films, it is reasonable to conclude that the oxidant is being provided by the ZnO—and therefore the oxygen within the lattice.

Corroboration of the ZnO thin film erosion was made by AAS analysis of the reaction liquid (Fig. 6). This confirms that this degradation is due to the Zn leaching out of the ZnO lattice, as Zn metal (Table 2 and Fig. 6) is detected in the reaction samples taken after 6 h in each case. When compared on a surface area normalised basis,

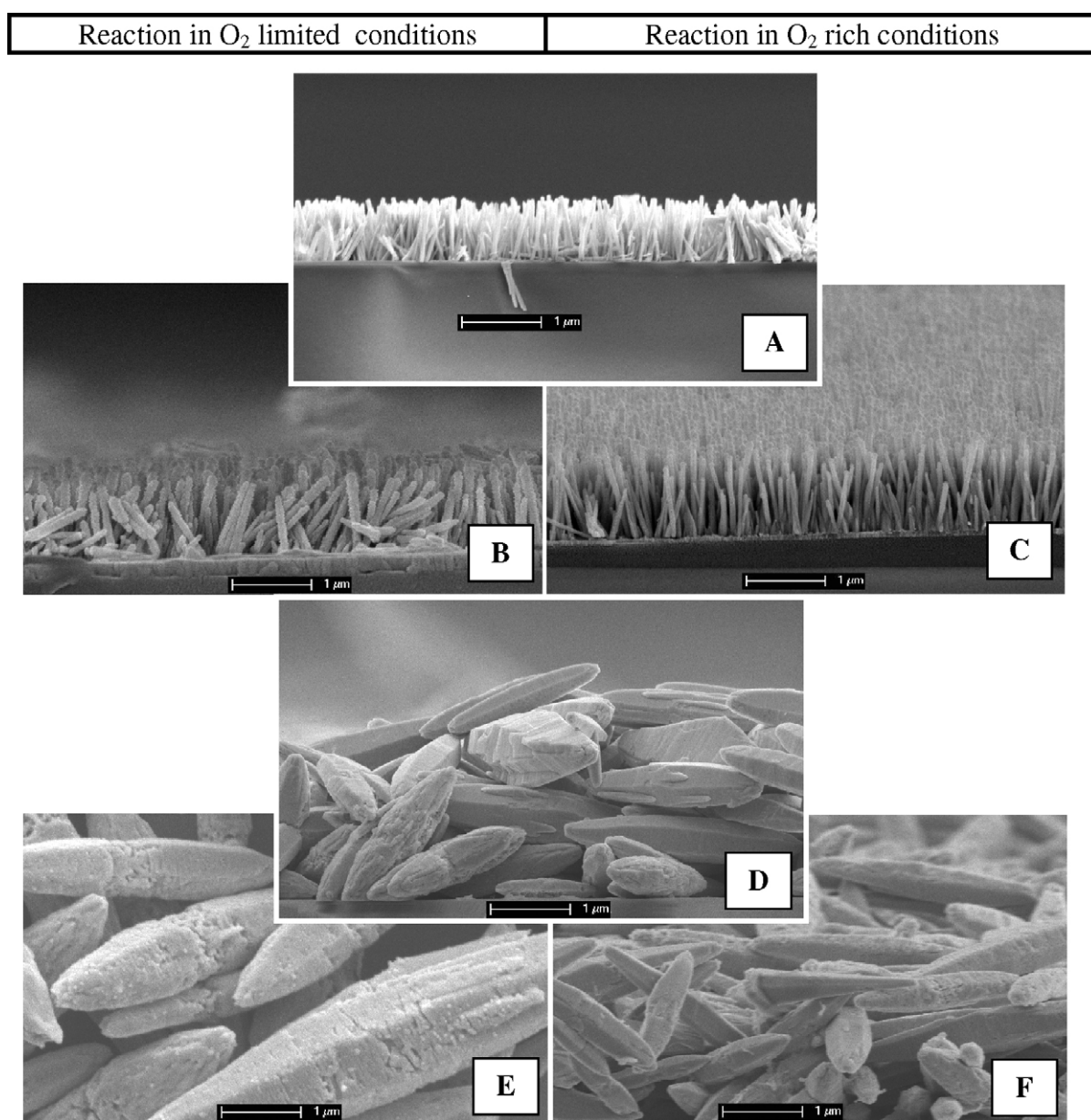


Fig. 4. Comparison of the solution 2 (S2) derived ZnO thin film surface morphologies using SEM imaging before and after Methylene Blue photocatalysed degradation: (A) S2-MS (un-reacted); (B) S2-MS (reacted with limited O₂); (C) S2-MS (reacted under O₂ rich conditions); (D) S2-CG (un-reacted); (E) S2-CG (reacted with limited O₂); (F) S2-CG (reacted under O₂ rich conditions).

Table 2
Concentration of zinc in reaction solutions as determined by atomic absorption spectroscopy (AAS), summarised as total zinc concentration (Zn; ppb) and zinc concentration normalised by the original surface area of the thin film catalyst it came from (Zn/SA; ppb/m²).

Thin film photo-catalyst	O ₂ limited conditions			O ₂ rich conditions			%Decrease Zn/SA ^a (ppb/m ²)
	Surface area (SA) (m ²)	Zn (ppb)	Zn/SA (ppb/m ²)	Surface area (SA) (m ²)	Zn (ppb)	Zn/SA (ppb/m ²)	
S1-MS	0.1296	9575	73,881	0.1296	4527	34,931	52.7
S1-CG	0.0599	7532	125,743	0.0599	5425	90,568	28.0
S2-MS	0.3427	7252	21,161	0.3427	5975	17,435	17.6
S2-CG	0.0445	6123	137,596	0.0445	4942	111,056	19.3
S3-MS	–	2131	–	–	1984	–	–
S3-CG	–	2204	–	–	2105	–	–

^a This is equivalent to % increase in thin film stability.

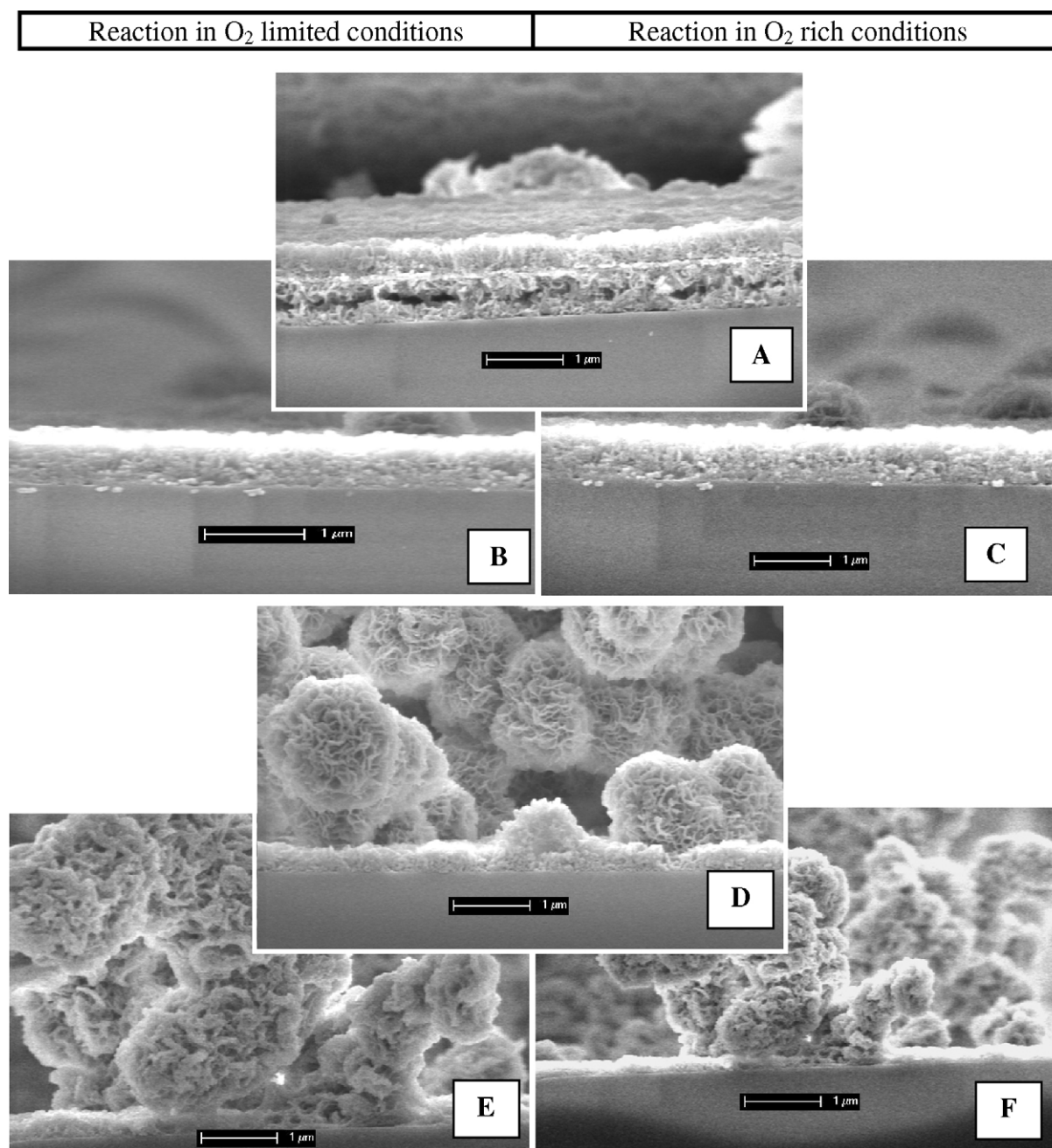


Fig. 5. Comparison of the solution 3 (S3) derived ZnO thin film surface morphologies from SEM imaging before and after Methylene Blue photocatalysed degradation: (A) S3-MS (un-reacted); (B) S3-MS (reacted with limited O₂); (C) S3-MS (reacted under O₂ rich conditions); (D) S3-CG (un-reacted); (E) S3-CG (reacted with limited O₂); (F) S3-CG (reacted under O₂ rich conditions).

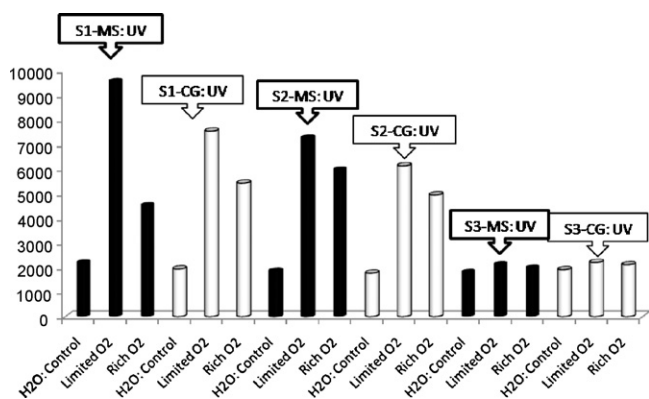


Fig. 6. Concentration of Zn metal in the final reaction liquid as measured by atomic absorption spectroscopy (AAS) for the reactions photocatalysed by the ZnO thin films derived from solutions S1 and S2 on both clean glass slides (CG) and magnetron sputtered templates (MS).

both template growth films (S1-MS and S2-MS) leached the least amount of zinc, with S2-MS being the most stable by a factor of 3.5. No significant change is noticed in the solution concentration of Zn for S3-MS and S3-CG (Fig. 6) before and after reaction under limited O₂ condition. This may indicate the erosion is caused by leaching of a component other than ZnO and combined with the low reaction rate seen from these films (Section 3.2) corroborates the hypothesis that the oxidant is being provided by the ZnO lattice (i.e. the low reaction rate is because there is little ZnO eroded).

Overall however, these results show that these films are not suitable for photocatalysis under oxygen limited conditions.

3.1.3. Morphology after reaction under oxygen rich conditions

To try to overcome this stability problem and to also determine the true reaction rate (i.e. the reaction is not mass transfer limited), experiments under oxygen rich conditions were conducted. Figs. 3C and F, 4C and F and 5C and F show the surface of the six different thin films after the photocatalytic oxidation of Methylene Blue under oxygen rich conditions. It can be observed that the structures of S1-MS, S1-CG, S2-MS and S2-CG are more intact and less hollowed out in comparison to the films used in oxygen limited conditions, showing that the presence of readily available oxygen (dissolved in the liquid) makes the thin films more stable and robust. No prominent change in surface morphologies of S3-MS (Fig. 5B and C) and S3-CG (Fig. 5E and F) were noticed both under oxygen limited and rich conditions however, indicating that the chemistry and/or morphology of the films from solution 3 (S3) are unstable to any photocatalytic process. As discussed in Section 3.1.2, this is most likely because something other than ZnO is leaching from the thin film lattice, causing the erosion. This is clearly not the case for the thin films produced from solutions 1 and 2 however.

AAS analysis of the reaction liquid (Fig. 6 and Table 2) confirms that all morphologies (S1-MS, S1-CG, S2-MS and S2-CG) show less dissolution of Zn under oxygen rich conditions as compared to oxygen limited reactions. Again very minute changes in Zn amount were calculated in S3-MS and S3-CG samples under oxygen rich reaction conditions (Table 2 and Fig. 6). Table 2 also shows that on a surface area basis, again the template growth films (S1-MS and S2-MS) show the least amount of Zn leaching, with S2-MS again leaching the least amount of Zn and therefore are the most stable under both oxygen limited and oxygen rich conditions. This perhaps indicates that the MS template either allows a more stable bond between the glass substrate and the ZnO film and/or the morphologies produced are less susceptible to leaching during photocatalysis. This may also indicate that PEI and deposition at pH 7.5 increases the binding of the ZnO and decreases the amount of Zn lost during reaction.

Overall, this result suggests that using oxygen rich conditions either minimises or prevents lattice oxygens from participating in the photocatalysed oxidation reaction, or replaces the lattice oxygen that are used in this reaction. This could indicate that photocatalysed oxidation of Methylene Blue by these ZnO thin films occurs (at least partially) by a Mars Van Krevelen type mechanism [29]. It is speculated that oxygen from the catalyst lattice is removed and used in the radical initiation and propagation phases of the photocatalytic reaction. The physical ZnO degradation observed in the oxygen limited experiments is because there is only a limited oxygen supply to replenish the lattice oxygens used. The catalyst degradation is therefore less in the presence of oxygen since the lattice oxygen's (and therefore the structure) can be regenerated. To the authors' knowledge, this study is the first evidence that a Mars Van Krevelen type mechanism could contribute to ZnO photocatalytic reactions. This could indicate that the photocatalysed oxidation reactions occur by a Mars Van Krevelen type mechanism (i.e. lattice oxygen are used for the oxidation, causing a degradation of the ZnO lattice over time). This has been seen before for titanium dioxide and other ZnO containing catalysts. For example, Lee and Falconer [30] show that lattice oxygens are extracted from titanium dioxide (Degussa P25) during the photocatalytic decomposition of formic acid and Ovesen et al. [31] attributed the change in particle morphology for a ZnO/Cu catalyst to a change in numbers of oxygen vacancies at the Zn-O interface. However, there is little evidence (until now) of the mechanism occurring in ZnO photocatalysis. Understanding the operating envelope of this mechanism could provide a pathway to stabilising these types of ZnO photocatalysts and thereby enable their possible application by Industry, so that the aforementioned economic [1,2] and performance [1,3] advantages over TiO₂ can be realized.

3.2. Relationships with photocatalytic activity

3.2.1. Reaction kinetics

Linear regression of the reaction data shows that the photocatalytic degradation of Methylene Blue follows the expected first order reaction kinetics for all reactions. Apparent first order reaction rate constants on a reaction liquid volume (V) basis (k_{app}) and UV exposed catalyst surface area (S_{ex}) basis (k'_{app}) are summarised in Table 3.

3.2.2. Oxygen limited conditions

Results show that there is a clear relationship between surface morphology (and the related thin film preparation method) and photocatalytic activity for these ZnO thin film supported catalysts. Fig. 7 shows that there is no difference in the photocatalytic activity between the S1-MS and S1-CG films despite that the surface area of S1-MS being approximately twice as large as the S1-CG surface area. This is confirmed in Table 3, where the rate constants k'_{app} were (4.11×10^{-9} and 8.8×10^{-9}) respectively. Since the film morphologies are different (S1-MS has vertically aligned 1.5–2 μm tall crystal and S1-CG has random stacks of both horizontal as well as vertical 2–2.5 μm crystals), this suggests that it is not the surface area which is the most important factor for photocatalytic activity, and film morphology has a significant influence, corroborating previous findings Wahi et al. [13] and Li and Haneda [17].

Due to three dimensional anfractuous woven structures of S3-MS and S3-CG it was very hard to calculate the approximate surface area. However on the basis of apparent rate constant k_{app} , S3-MS and S3-CG has more or less the same photocatalytic activity as S1-MS and S1-CG. The only difference is that thin films obtained from S3-MS is slightly more effective as S3-CG ($k_{app} = 8.0 \times 10^{-6} \text{ s}^{-1}$ and $k_{app} = 1.0 \times 10^{-6} \text{ s}^{-1}$).

Table 3

Summary of the 1st order reaction rate constants on a liquid volume basis (k_{app} ; s^{-1}) and a UV exposed surface area (S_{ex}) basis (k'_{app} ; $m^3 m^2 s^{-1}$) for the photocatalysed degradation of 5 mg L⁻¹ Methylene Blue.

Thin film photocatalyst	Estimated UV exposed surface area S_{ex} (m^2)	First order rate constants			
		O ₂ limited conditions		O ₂ rich conditions	
		k_{app} (s^{-1})	k'_{app} ($m^3 m^2 s^{-1}$)	k_{app} (s^{-1})	k'_{app} ($m^3 m^2 s^{-1}$)
S1-MS	0.1296	1.33×10^{-5}	4.11×10^{-9}	1.50×10^{-5}	4.60×10^{-9}
S1-CG	0.0599	1.33×10^{-5}	8.8×10^{-9}	8.33×10^{-6}	5.56×10^{-9}
S2-MS	0.3427	4.0×10^{-5}	4.66×10^{-9}	6.0×10^{-5}	7.0×10^{-9}
S2-CG	0.0445	1.50×10^{-5}	1.33×10^{-8}	1.66×10^{-5}	1.49×10^{-8}
S3-MS	–	8.0×10^{-6}	–	2.0×10^{-6}	–
S3-CG	–	1.0×10^{-6}	–	6.0×10^{-6}	–
ZnO powder	0.0714	1.03×10^{-4}	2.86×10^{-10}	–	–

In contrast, there is a clear difference in the photocatalytic activity between S2-MS and S2-CG films ($k'_{app} = 4.66 \times 10^{-9}$ and $1.33 \times 10^{-8} m^3 m^2 s^{-1}$ respectively, see Table 3). For the S2 films, S2-MS shows an increase in activity of about 2.7 times whilst the surface area is about 7 times larger. The S2-MS surface microstructure is a much smaller and more aligned structure (Fig. 4B), with a much larger surface area (Table 3) in comparison to the S2-CG slides (Fig. 4E). This shows that for S2 films, an increase in surface area and perhaps the more aligned structure will increase the photocatalytic activity, in agreement with previous research [12,14,15].

Comparing all the different morphologies, overall, S1-CG and S2-CG are more photocatalytically active (on a surface area basis). This could be attributed to these films being less stable and undergoing greater Zn leaching (Table 2 and Figs. 3 and 4), thereby supplying a greater amount of oxygen from the lattice to participate in the degradation of Methylene Blue. An additional explanation could be that different crystallographic surfaces are present in these more random structures and these surfaces are more photocatalytically active than those in the more aligned structures from MS template growth. This hypothesis is currently being tested.

3.2.3. Oxygen rich conditions

Photocatalytic activities of all different microstructures were also studied under oxygen rich conditions (Fig. 8 and Table 3). Unexpectedly, the additional oxygen affected the different thin films and morphologies quite differently.

The S2-MS and S2-CG thin films showed a significant increase in photocatalytic activity for the degradation of Methylene Blue under oxygen rich conditions, as expected, since studies have shown that the addition of oxygen as an electron acceptor gives a higher reaction rate than with having either a photocatalyst or oxygen on its own [31]. This may also indicate that the Mars Van Krevelen type

mechanism is less important when sufficient dissolved oxygen is available to photocatalysts derived from solution S2 and that the dissolved oxygen can be used in the photocatalytic reaction rather than the lattice oxygen from the ZnO thin film.

In contrast, for the S1-MS thin films, there was no significant difference in photocatalytic activity in comparison to the experiments performed under oxygen limited conditions. This may indicate that the rate limiting step was not related to the liquid phase dissolved oxygen concentration and perhaps a Mars Van Krevelen type mechanism where supply and replenishment of the lattice oxygens are key to the reaction rate for photocatalysts derived from solution 1. The extreme of this case is the S1-CG film, which has a lower photocatalytic activity than under oxygen limited conditions. However, this is most likely due to an uneven ZnO coating on the glass substrate surface, as the thin films prepared directly on glass substrate did not show an even structure throughout the film.

Photocatalytic activity of thin films obtained by using solution S3 again differ. S3-CG thin films have six times higher photocatalytic activity under oxygen rich condition. S3-MS showed little photocatalytic activity under oxygen rich conditions. Comparing this to the photocatalytic activity of S3-MS under oxygen limited conditions (Fig. 7), this could perhaps mean that the rich supply of dissolved oxygen for this film minimised the photocatalytic degradation of the Methylene Blue by minimising or preventing the lattice oxygens from participating in the reaction.

Comparing the three template growth films (S1-MS, S2-MS and S3-MS), shows that again there is a clear relationship between surface morphology (and the related thin film preparation method) and photocatalytic activity for these ZnO thin film supported catalysts, as there is a marked difference in photocatalytic activity (first order rate constant, $k_{app} = 1.33 \times 10^{-5}$, 4.0×10^{-5} , $8.0 \times 10^{-6} s^{-1}$

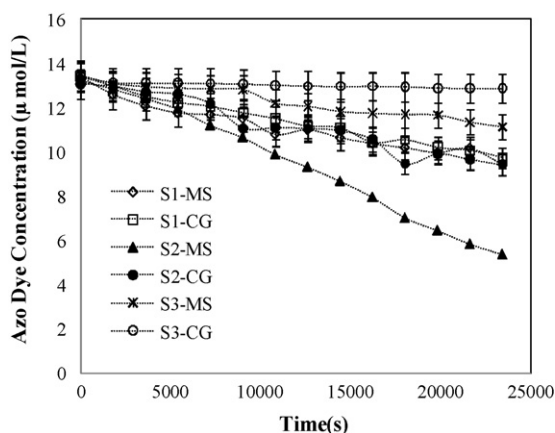


Fig. 7. Comparison of the degradation of Methylene Blue by the ZnO thin films derived from solutions S1, S2 and S3 under oxygen limited conditions.

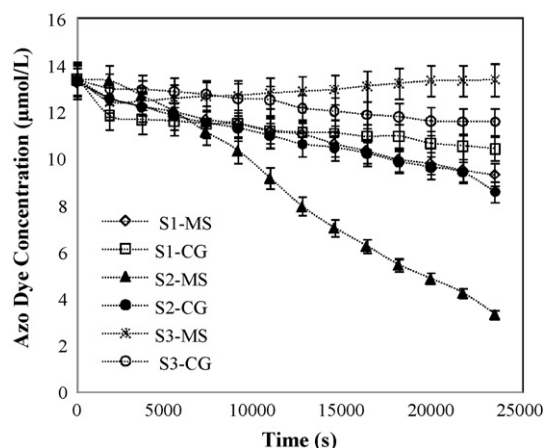


Fig. 8. Comparison of the degradation of Methylene Blue by the ZnO thin films derived from solutions S1, S2 and S3 under oxygen rich conditions.

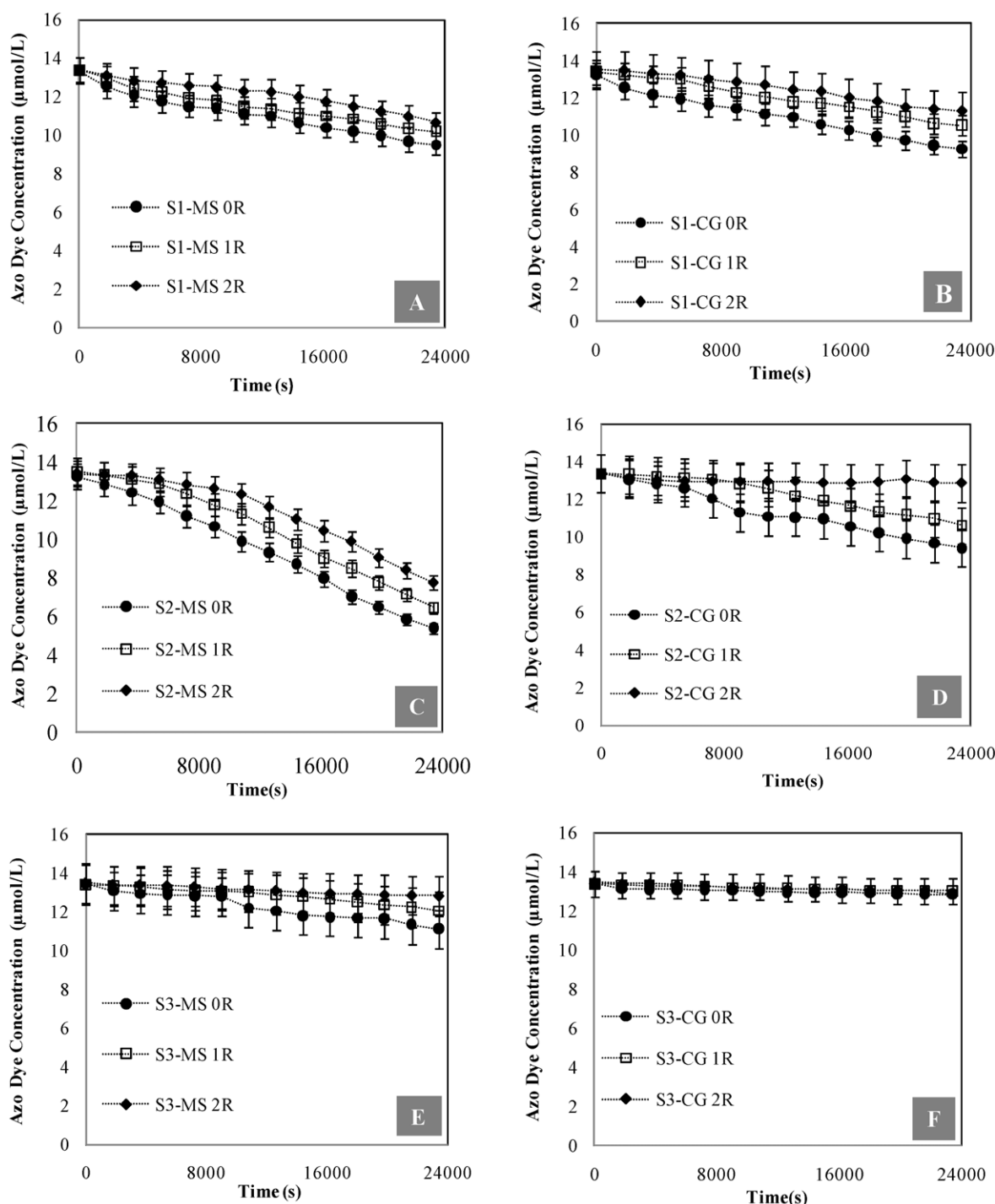


Fig. 9. Reusability and reproducibility of the ZnO thin films in the photocatalysed degradation of 5 mg L⁻¹ Methylene Blue under O₂ limited conditions. (A) S1-MS; (B) S1-CG; (C) S2-MS; (D) S2-CG; (E) S3-MS; (F) S3-CG, where 0R denotes initial use of a film, and 1R and 2R denote the first and second reuse of the same film respectively.

respectively; see Table 3). S2-MS has the highest photocatalytic activity, S1-MS, the second highest and the S3-MS has the lowest photocatalytic activity. S2-MS has a larger surface area than S1-MS, thus it is expected to have a larger photocatalytic activity. S3-MS has the smallest ZnO microstructure and therefore the least amount of ZnO surface area, therefore consistent with having the lowest volume-basis reaction rate. Furthermore, the alignment of the ZnO microstructure may be playing an important role. S1-MS and S2-MS films have ordered arrays of ZnO columns, grown from the substrate upwards (Fig. 2A and C). The shape and alignment of the S3-MS is quite different (Fig. 2E). XRD results [27] indicate that

for S1-MS at least, this higher reaction rate could very likely be due to the aligned columnar nano-rod structure. S1-MS has a sharply oriented crystalline ZnO structure, with one major peak was found at 34.4° which correlates to the (1 0 0) ZnO peak. Li et al. [32] state that the ZnO surface face exposed to the UV-light influences the photocatalytic activity, and so this aligned structure may therefore provide an orientation for maximising the redox reactions involved in the photocatalytic degradation. It may also be possible that the S2-MS immobilised ZnO structure also prevents the loss of ZnO lattice oxygen (in the Mars Van Krevelen type mechanism) as previously noted, indicating an increase in the catalysts stability due

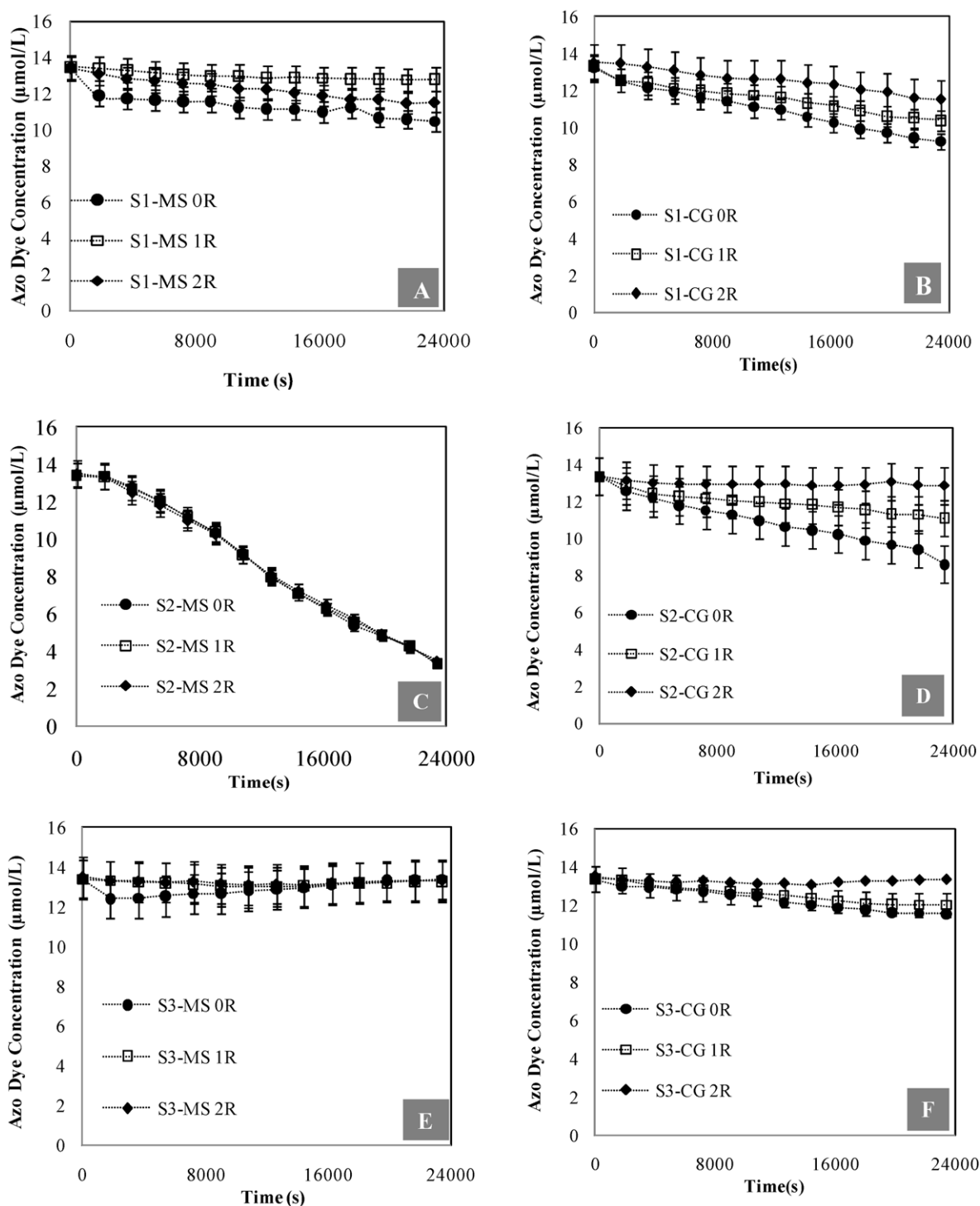


Fig. 10. Reusability and reproducibility of the ZnO thin films in the photocatalysed degradation of 5 mg L⁻¹ Methylene Blue under O₂ rich conditions, A) S1-MS; (B) S1-CG; (C) S2-MS; (D) S2-CG; (E) S3-MS; (F) S3-CG, where 0R denotes initial use of a film, and 1R and 2R denote the first and second reuse of the same film respectively.

to efficient formation of radicals that initiate and propagate the advanced oxidation degradation.

3.3. Reuseability of the thin films

In addition to ensuring the thin films have a sufficiently large UV exposed surface area and suitable morphology to maximise photocatalytic activity, a key property of any thin film catalyst is that it must be mechanically and chemically stable, retaining a high catalytic activity over an extended period of use and reuse. This is so

that use is viable: once it is coated on a support material within a reactor, it can remain there for an economically and practically viable time for the operation. Consequently, each film was reused in several reactions in order to determine the effect of these repeated uses on the photocatalytic activity and film morphology.

3.3.1. Oxygen limited conditions

Fig. 9 shows the effect of reusability of the films under limited oxygen conditions. One film of each morphology was reused three times for Methylene Blue degradation (referred to in Fig. 9 as 0R for

the initial use, and 1R and 2R for the first and second reuse respectively of the same film under the same reaction conditions). It can be observed that the photocatalytic activity decreases with each experimental run, showing that the catalyst is not suitable for multiple uses under oxygen limited conditions. This is in agreement with previous studies which have indicated a low stability of ZnO [22] and Figs. 3B and E, 4B and E, 5B and 6, showing that the surface is degraded by the reaction, which would decrease the surface area, crystallinity and aligned morphology, all of which decrease photocatalytic activity. Due to the very low photocatalytic activity of S3-CG (Fig. 9F) it was hard to visualise any effect on its multiple uses under the same reaction conditions. This low photocatalytic activity is consistent with the low levels of ZnO dissolution that indicates that the Mars Van Krevelen type mechanism is likely not prominent for photocatalysis with thin films derived from solution 3 (S3) as discussed in Section 3.1.2.

3.3.2. Oxygen rich conditions

Fig. 10 shows the effect of reusability of the films under oxygen rich conditions. For S1-MS, S1-CG, S2-CG, S3-MS and S3-CG similar results as under the oxygen limited conditions are observed. This is surprising, as the surface structure is visibly more intact (Figs. Fig. 3C and F, 4F, 5C and F) and there is significantly less ZnO dissolved in the liquid (Fig. 6). This confirms the previous observation that there is poorer binding between the glass substrate and solution deposited ZnO films than for the magnetron sputtered films. The poor reusability of S1-MS and S3-MS could also be the result

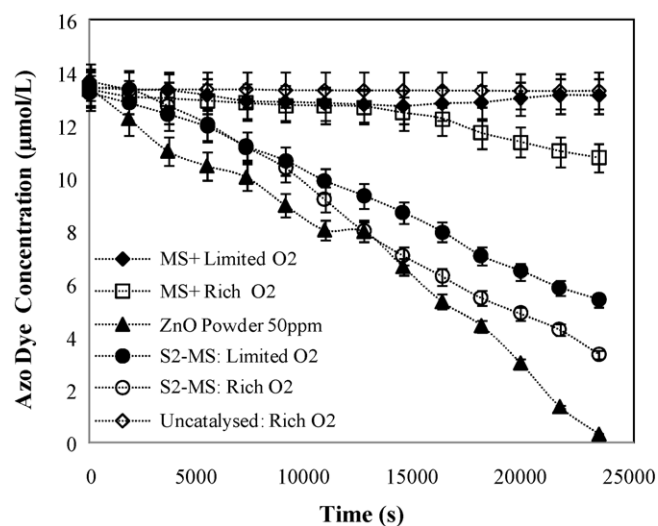


Fig. 11. Comparison of the photocatalytic activity of MS films to ZnO powder under both oxygen limited and oxygen rich conditions.

of these films only having a thin MS layer remaining after this multiple reuse. With solution S1 dissolving part of the MS layer during deposition of the top layer, as observed in Section 3.1.1, S1-MS has less MS template layer to bind to than S2-MS and are therefore less stable to reuse. The lack of stability of S3 films is most likely due to

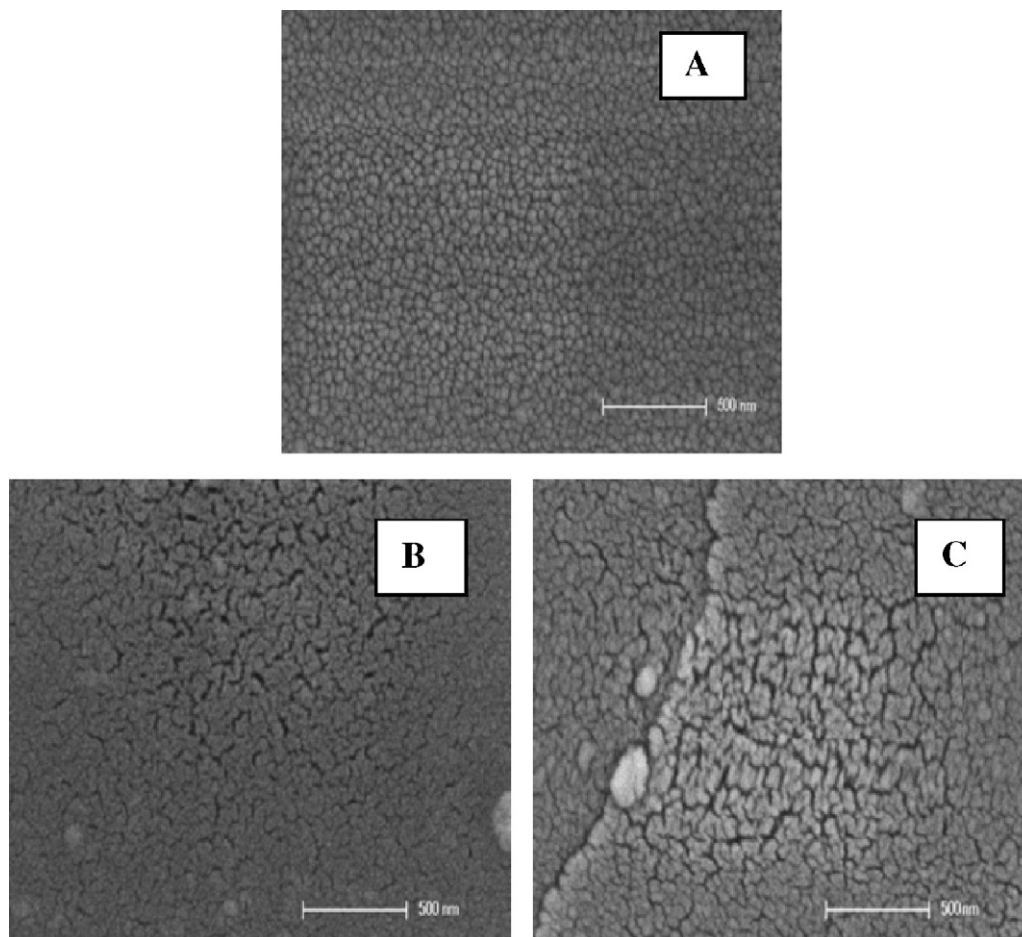


Fig. 12. The effect of photocatalytic reaction of Methylene Blue on the top surface morphology of the MS films using SEM imaging: (A) MS only; (B) MS film reacted under oxygen limited conditions O_2 ; (C) MS film reacted under oxygen rich conditions.

some leached component of S3, as discussed in Sections 3.1.2 and 3.1.3.

In contrast, the S2-MS thin film has an excellent reproducibility after multiple uses, showing no decrease in the photocatalytic activity after three runs. Again, this is the morphology that also showed the largest improvement under oxygen rich conditions. This again shows that morphology (and the thin film preparation method) influences photocatalytic activity as previously discussed.

Since thin film S2-MS was the most stable film for reuse and had the highest reaction rate of all of the films under both oxygen limited and oxygen rich conditions, the S2-MS photocatalytic activity was therefore compared to that of the benchmark ZnO catalysts and uncatalysed UV photolysis.

3.4. Comparison between S2-MS, ZnO MS films and ZnO powder

Fig. 11 shows the photocatalytic activity (under both limited and oxygen rich conditions, unless otherwise stated) of the S2-MS thin film was benchmarked against MS only films, commercially available ZnO powder and uncatalysed UV photolysis (under oxygen rich conditions only). MS only films showed no photocatalytic activity without oxygen, whilst under oxygen rich conditions showed some photocatalytic degradation of the Methylene Blue ($k_{app} = 9.0 \times 10^{-6} \text{ s}^{-1}$). Using a considerable mass of ZnO powder compared to that typically in the thin films (50 ppm powder, as this was the smallest mass that could be accurately measured and used with the 40 mL liquid reaction volume) allowed the Methylene Blue to be completely degraded during the observed reaction time at a comparatively large reaction rate on a liquid volume basis ($k_{app} = 1.0 \times 10^{-4} \text{ s}^{-1}$ and $k''_{app} = 2.86 \times 10^{-10} \text{ m}^3 \text{ m}^2 \text{ s}^{-1}$) under oxygen limited conditions.

The ZnO powder had the largest photoactivity for the mass added. This mass is greater than that added for the films hence this result is not surprising. A fairer basis of comparison is on a surface area basis. It can be seen from Table 3 that the ZnO powder had a lower photocatalytic activity based than the films based on the first order reaction rate constant per surface area basis. This indicates that the larger thin film structures (S1-MS, S1-CG, S2MS and S2-CG) might have a larger photocatalytic activity based on surface area. Further studies are required to investigate the mass to surface area influence.

Fig. 12 shows SEM images of the top surface of the unreacted MS film before and after reaction under limited and oxygen rich conditions. In contrast to the solution growth films, no obvious structural effect is observed on films after reactions under oxygen limited conditions, which is in agreement with the lack of photocatalytic activity. Since the reaction does not significantly change the microstructure nor any material deposition of model compound MB at its surfaces, it can be concluded that these MS deposited films may not be able to use lattice oxygens and undergo photocatalysed oxidation using a Mars Van Krevelen type mechanism. Therefore it may be either the morphology formed and/or the components used in the hydrothermal solution deposition ZnO thin film growth method that enable the oxygens within the lattice to be available for the S1 and S2 ZnO thin films. This result is further confirmed by the images after reaction under oxygen rich conditions, which show that although the structure displays cracks (which are most likely the result of mechanical forces during use and reaction rather than an artefact caused by the reaction), overall there is little change in the underlying structure of the MS films. Consequently, it can be concluded that it is the hydrothermally solution deposited ZnO nanostructured thin films S1 and S2 that are photocatalytically oxidising the Methylene Blue via a Mars Van Krevelen type mechanism. Further work is continuing to determine the structural and chemical reasons for this.

4. Conclusions

This work has shown the following:

- The ZnO films prepared are effective as photocatalysts for the liquid-phase photo-oxidation of Methylene Blue in oxygen limited and/or oxygen rich conditions. The Methylene Blue removal for the ZnO thin film slides varied between 0% and 75% after 6 h photolysis.
- A clear relationship between surface morphology (and the related thin film preparation method) and photocatalytic activity was observed for hydrothermally solution deposited ZnO thin film supported catalysts: the tallest, most aligned structure had the highest photocatalytic activity (S2-MS; 60% MB removal after 6 h photolysis in oxygen limited conditions and 75% in under oxygen rich conditions), whilst the smallest, least aligned structure had the lowest photocatalytic activity (S1-CG).
- For the thin films grown from solutions containing $\text{Zn}(\text{NO}_3)_2$ + HMT and $\text{Zn}(\text{NO}_3)_2$ + HMT + PEI (solutions 1 and 2 respectively), a rich supply of oxygen decreases the structural erosion during the photoreaction with Methylene Blue. This suggests that the photocatalysed oxidation by these solution deposited ZnO thin films occurs (at least partially) by a Mars Van Krevelen type mechanism. This would mean that oxygen from the catalyst lattice is removed and used in the oxidation reaction. The physical ZnO degradation observed in the oxygen limited experiments could therefore be because there is only a limited supply of oxygen to replenish the lattice oxygens used. The physical degradation of the catalyst is therefore diminished in the presence of oxygen, since the lattice oxygens (and therefore the catalyst structure) can be regenerated.

Future work is therefore concentrated on increasing both the durability and activity of the S2-MS nano-rod thin films and exploring the stable operating envelope around loss of ZnO through a possible Mars Van Krevelen mechanism. This may finally provide a pathway enabling the application of ZnO photocatalysts by Industry and allowing the previously reported practical and economic advantages over titanium oxide [1–3] to be realised.

Acknowledgements

The authors would like to thank the Higher Education Commission (HEC) of Pakistan for funding Arshid Mahmood Ali's scholarship. The authors also thank the University of Auckland for supporting this work with grants (3607612/9271 and 3609556/9271), as well as the Department of Chemical and Materials Engineering at the University of Auckland for funding consumables. The authors would also like to acknowledge Wei Gao, Xiaodong Yan, Muhammad Shameem, Catherine Hobbs, Laura Liang, Alan Clendinning and Abel Francis for their help in this work.

References

- [1] B. Dindar, S. Içli, J. Photochem. Photobiol. A 140 (2001) 263–268.
- [2] N. Daneshvar, D. Salari, A.R. Khataee, J. Photochem. Photobiol. A 162 (2004) 317–322.
- [3] A. Akyol, H.C. Yatmaz, M. Bayramoglu, Appl. Catal. B 54 (2004) 19–24.
- [4] K. Kabra, R. Chaudhary, R.L. Sawhney, Ind. Eng. Chem. Res. 43 (2004) 7683–7696.
- [5] K. Eufinger, D. Poelman, H. Poelman, R.D. Gryse, G.B. Marin, J. Phys. D: Appl. Phys. (2007) 5232.
- [6] A. Mills, J. Wang, M. Crow, G. Taglioni, L. Novella, J. Photochem. Photobiol. A 187 (2007) 370–376.
- [7] Y. Xiang, L. Zhengwei, C. Ruiqun, G. Wei, Cryst. Growth Des. 8 (2008) 2406–2410.
- [8] P.V. Kamat, R. Huehn, R. Nicolaescu, J. Phys. Chem. B 106 (2002) 788–794.
- [9] J.L. Yang, S.J. An, W.I. Park, G.-C. Yi, W. Choi, Adv. Mater. 16 (2004) 1661–1664.
- [10] Z.W. Li, W. Gao, R.J. Reeves, Surf. Coat. Technol. 198 (2005) 319–323.

- [11] J. Lee, W. Gao, Z. Li, M. Hodgson, J. Metson, H. Gong, U. Pal, *Appl. Phys. A: Mater. Sci. Process.* 80 (2005) 1641–1646.
- [12] C. Hariharan, *Applied Catalysis A: General* 304 (2006) 55–61.
- [13] R.K. Wahi, W.W. Yu, Y. Liu, M.L. Mejia, J.C. Falkner, W. Nolte, V.L. Colvin, *J. Mol. Catal. A: Chem.* 242 (2005) 48–56.
- [14] S. Park, J.C. Lee, D.W. Lee, J.H. Lee, *J. Mater. Sci.* 38 (2003) 4493–4497.
- [15] F.M. Moghaddam, H. Saeidian, *Mater. Sci. Eng. B* 139 (2007) 265–269.
- [16] X. Wang, P. Hu, F.L. Yuan, L.J. Yu, *J. Phys. Chem. C* 111 (2007) 6706–6712.
- [17] D. Li, H. Haneda, *Chemosphere* 51 (2003) 129–137.
- [18] X. Li, K. Lv, K. Deng, J. Tang, R. Su, J. Sun, L. Chen, *Mater. Sci. Eng. B* 158 (2009) 40–47.
- [19] H. Li, Z. Bian, J. Zhu, D. Zhang, G. Li, Y. Huo, H. Li, Y. Lu, *J. Am. Chem. Soc.* 129 (2007) 8406–8407.
- [20] L. Xu, Y.-L. Hu, C. Pelligra, C.-H. Chen, L. Jin, H. Huang, S. Sithambaram, M. Aindow, R. Joesten, S.L. Suib, *Chem. Mater.* 21 (2009) 2875–2885.
- [21] S. Bakardjieva, V. Stengl, L. Szatmary, J. Subrt, J. Lukac, N. Murafa, D. Niznansky, K. Cizek, J. Jirkovsky, N. Petrova, *J. Mater. Chem.* 16 (2006) 1709–1716.
- [22] R.B.M. Cross, M.M.D. Souza, *Appl. Phys. Lett.* 89 (2006) 263513.
- [23] W. Gao, Z. Li, *Ceram. Int.* 30 (2004) 1155–1159.
- [24] A. Houas, H. Lachheb, M. Ksibi, E. Elaloui, C. Guillard, J.-M. Herrmann, *Appl. Catal. B* 31 (2001) 145–157.
- [25] S. Chakrabarti, B.K. Dutta, *J. Hazard. Mater.* 112 (2004) 269–278.
- [26] K. Byrappa, A. Subramani, S. Ananda, K. Rai, R. Dinesh, M. Yoshimura, *Bull. Mater. Sci.* 29 (2006) 433–438.
- [27] C.J. McFarlane, E.A.C. Emanuelsson, A.M. Ali, W. Gao, D.A. Patterson, *Optimising Zinc Oxide Nanostructured Thin Films as Photocatalyst for Industrial Wastewaters*, Proceedings of Chemeca 2009, Burswood Entertainment Complex, Perth, Australia, 2009, pp. 1–17.
- [28] Z.R. Tian, J.A. Voigt, J. Liu, B. McKenzie, M.J. McDermott, M.A. Rodriguez, H. Konishi, H. Xu, *Nat. Mater.* 2 (2003) 821–826.
- [29] K. Ramesh, L. Chen, F. Chen, Y. Liu, Z. Wang, Y.-F. Han, *Catal. Today* 131 (2008) 477–482.
- [30] G.D. Lee, J.L. Falconer, *Catal. Lett.* 70 (2000) 145–148.
- [31] C.V. Ovesen, B.S. Clausen, J. Schiøtz, P. Stoltze, H. Topsøe, J.K. Nørskov, *J. Catal.* 168 (1997) 133–142.
- [32] D. Li, H. Haneda, N. Ohashi, N. Saito, S. Hishita, *Thin Solid Films* 486 (2005) 20–23.